

QCD thermodynamics and confinement from a dynamical quasiparticle point of view

W. Cassing^{a,*}

^a*Institut für Theoretische Physik, Universität Giessen, Heinrich-Buff-Ring 16,
D-35392 Giessen, Germany*

Abstract

In this study it is demonstrated that a simple picture of the QCD gluon liquid emerges in the dynamical quasiparticle model that specifies the active degrees of freedom in the time-like sector and yields a potential energy density in the space-like sector. By using the time-like gluon density (or scalar gluon density) as an independent degree of freedom - instead of the temperature T as a Lagrange parameter - variations of the potential energy density lead to effective mean-fields for time-like gluons and an effective gluon-gluon interaction strength at low density. The latter yields a simple dynamical picture for the gluon fusion to color neutral glueballs when approaching the phase boundary from a temperature higher than T_c and paves the way for an off-shell transport theoretical description of the parton dynamics.

Key words: Quark gluon plasma, General properties of QCD, Relativistic heavy-ion collisions

PACS: 12.38.Mh, 12.38.Aw, 25.75.-q

1 Introduction

The formation of a quark-gluon plasma (QGP) and its transition to interacting hadronic matter – as occurred in the early universe – has motivated a large community for several decades (cf. [1] and Refs. therein). Early concepts of the QGP were guided by the idea of a weakly interacting system of partons (quarks, antiquarks and gluons) since the entropy s and energy density ϵ were found in lattice QCD to be close to the Stefan Boltzmann (SB) limit for a relativistic noninteracting system [2]. However, this notion had to be given up in the last years since experimental

* corresponding author

Email address: Wolfgang.Cassing@theo.physik.uni-giessen.de (W. Cassing).

observations at the Relativistic Heavy Ion Collider (RHIC) indicated that the new medium created in ultrarelativistic Au+Au collisions was interacting more strongly than hadronic matter. Moreover, in line with earlier theoretical studies in Refs. [3–5] the medium showed phenomena of an almost perfect liquid of partons [6,7] as extracted from the strong radial expansion and elliptic flow of hadrons as well the scaling of the elliptic flow with parton number *etc.* The latter collective observables have been severely underestimated in conventional string/hadron transport models [8–10], but hydrodynamical approaches did quite well in describing (at midrapidity) the collective properties of the medium generated during the early times for low and moderate transverse momenta [11,12]. Soon the question came up about the constituents of this liquid; it might be some kind of i) "epoxy" [13], i.e. a system of resonant or bound gluonic states with large scattering length, ii) a system of chirally restored mesons, instanton molecules or equivalently giant collective modes [14], iii) a system of colored bound states of quarks q and gluons g , i.e. gq , qq , gg *etc.* [15], iv) some 'string spaghetti' or 'pasta' *etc.* In short, many properties of the new phase are still under debate and practically no dynamical concepts are available to describe the freezeout of partons to color neutral hadrons that are subject to experimental detection.

Lattice QCD (lQCD) calculations provide some guidance to the thermodynamic properties of the partonic medium close to the transition at a critical temperature T_c up to a few times T_c , but lQCD calculations for transport coefficients presently are not accurate enough [16] to allow for firm conclusions. Furthermore, it is not clear whether the partonic system really reaches thermal and chemical equilibrium in ultrarelativistic nucleus-nucleus collisions and nonequilibrium models are needed to trace the entire collision history. The available string/hadron transport models [17–19] are not accurate enough - as pointed out above - nor do partonic cascade simulations [20–23] (propagating massless partons) sufficiently describe the reaction dynamics when employing cross sections from perturbative QCD (pQCD). This also holds - to some extent - for the Multiphase Transport Model AMPT [24] since it includes only on-shell massless partons in the partonic phase as in Ref. [21]. The same problem comes about in the parton cascade model of Xu and Greiner [25] where additional $2 \leftrightarrow 3$ processes like $gg \leftrightarrow ggg$ are incorporated. On the other hand it is well known that strongly interacting quantum systems require descriptions in terms of propagators D with sizeable selfenergies Π for the relevant degrees of freedom. Whereas the real part of the selfenergy gives contributions to the energy density, the imaginary parts of Π provide information about the lifetime and/or reaction rate of time-like 'particles' [4]. In principle, off-shell transport equations are available in the literature [26–28], but have been applied only to dynamical problems where the width of the quasiparticles stays moderate with respect to the pole mass [29]. On the other hand, the studies of Peshier [30,31] indicate that the effective degrees of freedom in a partonic phase should have a width γ in the order of the pole mass M already slightly above T_c .

The present study addresses essentially three questions: i) Do we understand the

QCD thermodynamics in terms of dynamical quasiparticles down to the phase boundary in a 'top down' scenario and what are the effective degrees of freedom as well as energy contributions? ii) Can such a quasiparticle approach help in defining an off-shell transport model that - at least in thermal equilibrium - reproduces the thermodynamic results from lQCD? iii) Are there any perspectives in modeling the transition from partonic to hadronic degrees of freedom in a dynamical way?

The present work is exploratory in the sense that it is restricted to a pure gluonic system of $N_c^2 - 1$ gluons with two transverse polarisations, i.e. degeneracy $d_g = 16$ for the gluonic quasiparticles that are treated as relativistic scalar fields. Note, however, that the qualitative features stay the same when adding light quark degrees of freedom [31]; this finding is well in line with the approximate scaling of thermodynamic quantities from lQCD when dividing by the number of degrees of freedom and scaling by the individual critical temperature T_c which is a function of the different number of parton species [32].

The outline of the paper is as follows: After a short recapitulation of the dynamical quasiparticle model in Section 2 new results on the space-like and time-like parts of observables are presented that allow for a transparent physical interpretation. In Section 3 we will examine derivatives of the space-like part of the quasiparticle energy density with respect to the time-like (or scalar) density which provides information on gluonic mean fields and their effective interaction strength. The implications of these findings with respect to an off-shell transport description are pointed out throughout the study. A summary and extended discussion closes this work in Section 4.

2 Off-shell elements in the DQPM

2.1 Reminder of the DQPM

The Dynamical QuasiParticle Model (DQPM)¹ adopted here goes back to Peshier [30,31] and starts with the entropy density s in the quasiparticle limit [33],

$$s^{dqp} = -d_g \int \frac{d\omega}{2\pi} \frac{d^3p}{(2\pi)^3} \frac{\partial n}{\partial T} \left(\text{Im} \ln(-\Delta^{-1}) + \text{Im} \Pi \text{Re} \Delta \right), \quad (1)$$

where $n(\omega/T) = (\exp(\omega/T) - 1)^{-1}$ denotes the Bose distribution function, Δ stands for the scalar quasiparticle propagator and Π for the quasiparticle selfenergy which is considered here to be a Lorentz scalar. In principle, the latter quantities are Lorentz tensors and should be evaluated in a nonperturbative framework. However, a more

¹ DQPM also stands alternatively for Dynamical-Quasiparticle-Peshier-Model

practical procedure is to use a physically motivated *Ansatz* with a Lorentzian spectral function,

$$\rho(\omega) = \frac{\gamma}{E} \left(\frac{1}{(\omega - E)^2 + \gamma^2} - \frac{1}{(\omega + E)^2 + \gamma^2} \right), \quad (2)$$

and to fit the few parameters to results from lQCD. With the convention $E^2(\mathbf{p}) = \mathbf{p}^2 + M^2 - \gamma^2$, the parameters M^2 and γ are directly related to the real and imaginary parts of the corresponding (retarded) self-energy, $\Pi = M^2 - 2i\gamma\omega$. It should be stressed that the entropy density functional (1) is not restricted to quasiparticles of low width γ and thus weakly interacting particles. In fact, in the following it will be shown that a novel picture of the hot gluon liquid emerges because γ becomes comparable to the quasiparticle mass already slightly above T_c [30,31].

Following [34] the quasiparticle mass (squared) is written in (momentum-independent) perturbative form,

$$M^2(T) = \frac{N_c}{6} g^2 T^2, \quad (3)$$

with a running coupling (squared),

$$g^2(T/T_c) = \frac{48\pi^2}{11N_c \ln(\lambda^2(T/T_c - T_s/T_c)^2)}, \quad (4)$$

which permits for an enhancement near T_c [34,35]. It will be shown below that an infrared enhancement of the coupling - as also found in the lQCD calculations in Ref. [36] for the long range part of the $q - \bar{q}$ potential - is directly linked to the gluon fusion/clustering scenario. In order to quantify this statement the coupling $\alpha_s(T) = g^2(T)/(4\pi)$ is shown in Fig. 1 as a function of T/T_c in comparison to the long range part of the strong coupling as extracted from Ref. [36] from the free energy of a quark-antiquark pair in quenched lQCD. For this comparison the actual parameters $\lambda = 2.42$, $T_s/T_c = 0.46$ have been adopted as in Ref. [4]. The parametrization (4) is seen to follow the lQCD results - also indicating a strong enhancement close to T_c - as a function of temperature reasonably well. One should recall that any extraction of coupling constants $\alpha_s(T)$ from lQCD is model dependent and deviations from (or agreement with) lattice 'data' have to be considered with care. The argument here is that the specific 'parametric form' of Eq. (4) is not in conflict with lQCD and that the coupling α_s and consequently the quasiparticle mass $M(T)$ has the right order of magnitude.

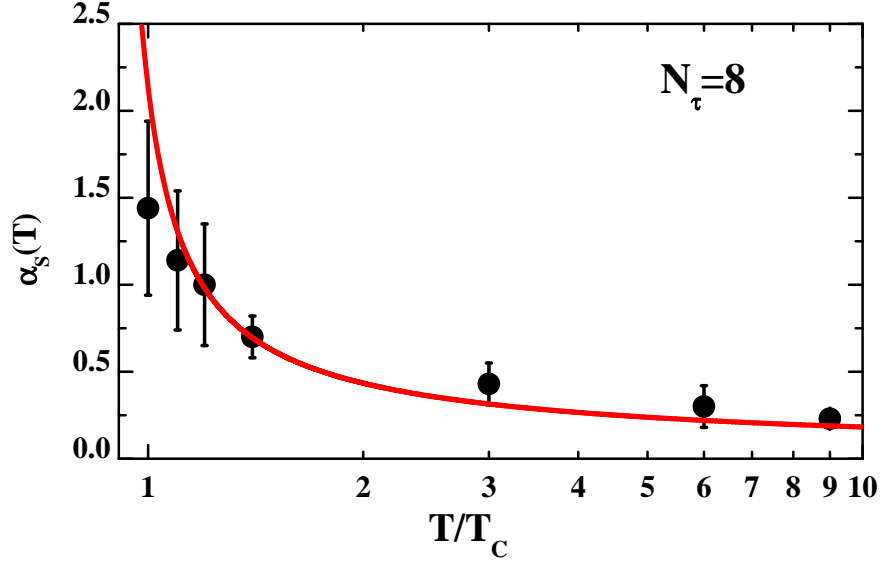


Fig. 1. The coupling $\alpha_s(T) = g^2(T)/(4\pi)$ (solid red line) as a function of T/T_c in comparison to the long range part of the strong coupling as extracted from Ref. [36] from the free energy of a quark-antiquark pair in quenched IQCD (for $N_\tau = 8$).

The width γ is adopted in the form $\gamma \sim g^2 T \ln g^{-1}$ [37] or, equivalently, in terms of M [30], as

$$\gamma(T) = \frac{3}{4\pi} \frac{M^2(T)}{T^2} T \ln \frac{c}{(M(T)/T)^2}, \quad (5)$$

where $c = 14.4$ (from [4]) is related to a magnetic cut-off. In case of the pure Yang-Mills sector of QCD the physical processes contributing to the width γ are both $gg \leftrightarrow gg$ scattering as well as splitting and fusion reactions $gg \leftrightarrow g$ or $gg \leftrightarrow ggg$, $ggg \leftrightarrow gggg$ etc. Note that the ratio $\gamma(T)/M(T) \sim g \ln(c/g^2)$ approaches zero only asymptotically for $T \rightarrow \infty$ such that the width of the quasiparticles is comparable to the mass for all practical energy scales on earth; the ratio $\gamma(T)/M(T)$ drops below 0.5 only for temperatures $T > 1.25 \cdot 10^5 T_c$ (for the parameters given above).

For the choice (2) for the spectral function the scalar effective propagator reads,

$$\Delta^{dqp}(\omega, \mathbf{p}) = \frac{1}{\omega^2 - \mathbf{p}^2 - M^2 + 2i\gamma\omega}, \quad (6)$$

which can easily be separated into real and imaginary parts. The entropy density (1) then reads explicitly [31],

$$s^{dqp}(T) = d_g \int \frac{d^3p}{(2\pi)^3} \left(-\ln(1 - e^{-\omega_p/T}) + \frac{\omega_p}{T} n(\omega_p/T) \right) + d_g \int \frac{d\omega}{2\pi} \frac{d^3p}{(2\pi)^3} \frac{\partial n}{\partial T} \left(\arctan\left(\frac{2\gamma\omega}{\omega_p^2 - \omega^2}\right) - \frac{2\gamma\omega(\omega_p^2 - \omega^2)}{(\omega_p^2 - \omega^2)^2 + 4\gamma^2\omega^2} \right), \quad (7)$$

using $\omega_p = \sqrt{\mathbf{p}^2 + M^2}$. The first line in (7) corresponds to the familiar on-shell quasiparticle contribution s_0 while the second line in (7) corresponds to the contribution originating from the finite width γ of the quasiparticles and is positive throughout but subleading (see below).

The pressure P now can be evaluated from

$$s = \frac{\partial P}{\partial T} \quad (8)$$

by integration of s over T , where from now on we identify the 'full' entropy density s with the quasiparticle entropy density s^{dap} . Note that for $T < T_c$ the entropy density drops to zero (with decreasing T) due to the high quasiparticle mass and the width γ vanishes as well because the interaction rate in the very dilute quasiparticle system becomes negligible. Since the pressure for infinitely heavy (noninteracting) particles also vanishes the integration constant for the pressure P - when integrating (8) - may safely be assumed to be zero, too.

The energy density ϵ then follows from the thermodynamical relation [34,38]

$$\epsilon = Ts - P \quad (9)$$

and thus is also fixed by the entropy $s(T)$ as well as the interaction measure

$$W(T) := \epsilon(T) - 3P(T) = Ts - 4P \quad (10)$$

that vanishes for massless and noninteracting degrees of freedom.

In Ref. [4] a detailed comparison has been presented with the lattice results from Ref. [39] for the pure gluonic sector to the quasiparticle entropy density (7) for the parameters given above. The agreement with the lattice data is practically perfect [4,30]. Needless to point out that also $P(T)$, $\epsilon(T)$ and $W(T)$ well match the lattice QCD results for $1 \leq T/T_c \leq 4$ [4,31] due to thermodynamical consistency. The same parameters are also adopted for the following calculations.

2.2 Time-like and space-like quantities

For the further argumentation it is useful to introduce the shorthand notation

$$\tilde{\Gamma}_P^\pm \dots = d_g \int \frac{d\omega}{2\pi} \frac{d^3p}{(2\pi)^3} 2\omega \rho(\omega) \Theta(\omega) n(\omega/T) \Theta(\pm P^2) \dots \quad (11)$$

with $P^2 = \omega^2 - \mathbf{p}^2$ denoting the invariant mass squared. The $\Theta(\pm P^2)$ function in (11) separates time-like quantities from space-like quantities and can be inserted for

any observable of interest.

As the first quantity we consider the entropy density (7). Its time-like contribution is almost completely dominated by the first line in (7) - that corresponds to the on-shell quasiparticle contribution s_0 - but also includes a small contribution from the second line in (7) which is positive for T below about $1.5 T_c$ and becomes negative for larger temperature. This time-like part s^+ is shown in Fig. 2 by the dotted blue line (multiplied by $(T_c/T)^3$). The second line in (7) - as mentioned above - corresponds to the contribution originating from the finite width γ of the quasiparticles and also has a space-like part s^- which is dominant (for the second line in (7)) and displayed in Fig. 2 by the lower red line (multiplied by $(T_c/T)^3$). Though s^- is subleading in the total entropy density $s = s^+ + s^-$ (thick solid green line in Fig. 2) it is essential for a proper reproduction of $s(T)$ close to T_c (cf. [31]). Note that the total entropy density s is not very different from the Stefan Boltzmann entropy density s_{SB} for $T > 2T_c$ as shown in Fig. 2 by the upper thin line (multiplied by $(T_c/T)^3$).

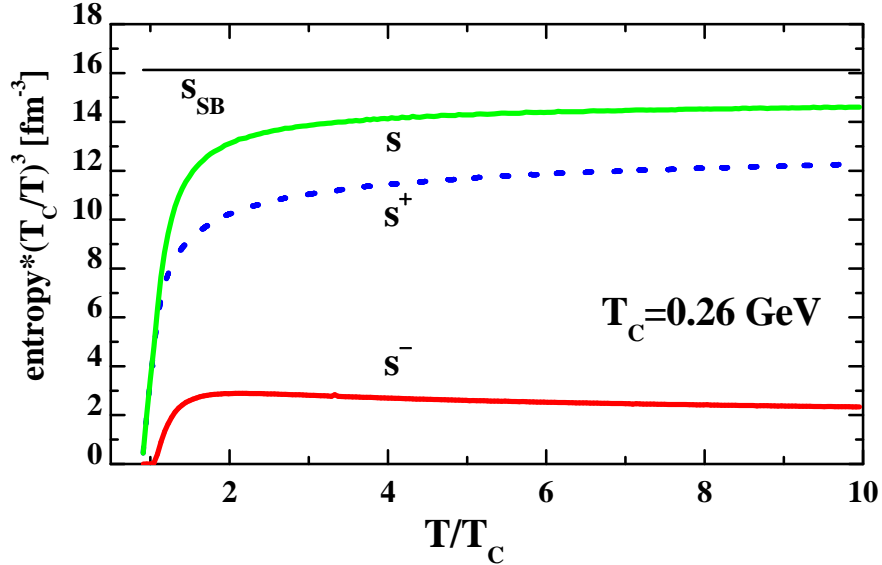


Fig. 2. The time-like contribution to the entropy density s^+ (dotted blue line), the space-like contribution s^- (lower red line) and the total entropy density $s = s^+ + s^-$ (thick solid green line) as a function of T/T_c . All quantities have been multiplied by the dimensionless factor $(T_c/T)^3$ assuming $T_c = 0.26$ GeV for the pure gluonic system [40]. The upper solid black line displays the Stefan Boltzmann limit s_{SB} for reference.

Further quantities of interest are the quasiparticle 'densities'

$$N^\pm(T) = \tilde{\text{Tr}}^\pm 1 \quad (12)$$

that correspond to the time-like (+) and space-like (-) parts of the integrated distribution function. Note that only the integral of N^+ over space has a particle number interpretation. In QED this corresponds to time-like photons (γ^*) which are virtuell

in intermediate processes but can also be seen asymptotically by dileptons (e.g. e^+e^- pairs) due to the decay $\gamma^* \rightarrow e^+e^-$ [17].

A scalar density N_s , which is only defined in the time-like sector, is given by

$$N_s(T) = \tilde{\text{Tr}}^+ \left(\frac{\sqrt{P^2}}{\omega} \right) \quad (13)$$

and has the virtue of being Lorentz invariant. Moreover, a scalar density can easily be computed in transport approaches for bosons and fermions [17,41] which is of relevance for the argumentation in Section 3.

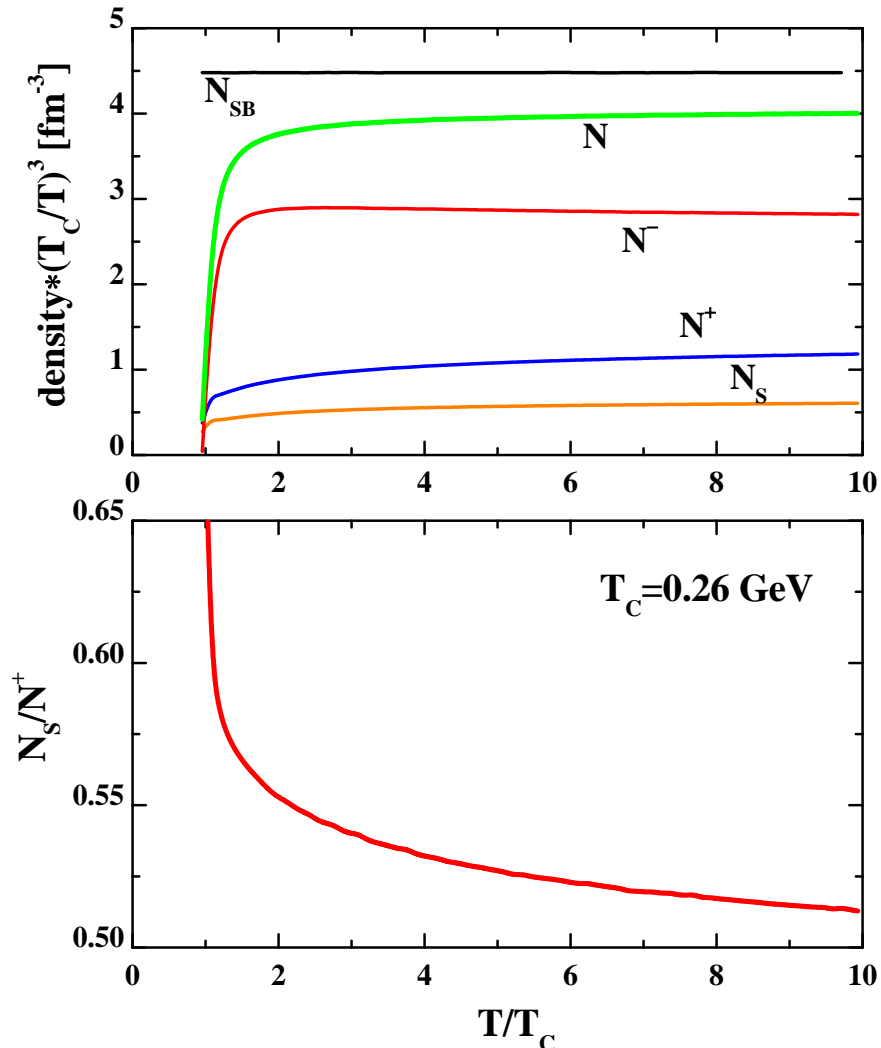


Fig. 3. Upper part: The scalar density N_s (lower orange line), the time-like density N^+ (blue line), the space-like quantity N^- (red line) and the sum $N = N^+ + N^-$ (thick solid green line) as a function of T/T_c assuming $T_c = 0.26$ GeV for the pure gluonic system [40]. The upper solid black line displays the Stefan Boltzmann limit N_{SB} for reference. All quantities are multiplied by the dimensionless factor $(T_c/T)^3$. Lower part: The ratio of the scalar density N_s to the time-like density N^+ as a function of the scaled temperature T/T_c .

The actual results for the different 'densities' (multiplied by $(T_c/T)^3$) are displayed in the upper part of Fig. 3 where the lower orange line represents the scalar density N_s , the blue line the time-like density N^+ , the red line the space-like quantity N^- and the thick solid green line the sum $N = N^+ + N^-$ as a function of T/T_c assuming (as before) $T_c = 0.26$ GeV for the pure gluonic system [40]. It is seen that N^+ is substantially smaller than N^- in the whole temperature range up to $10 T_c$ where it is tacitly assumed that the DQPM also represents lQCD results for $T > 4T_c$, which is not proven explicitly, but might be expected due to the proper weak coupling limit of (3), (5) (cf. Fig. 1). The application of the DQPM to $10 T_c$ is presented in Fig. 3 since the initial state at Large Hadron Collider (LHC) energies might be characterized by a temperature above $4 T_c$; note that the properties of the partonic phase will be explored from the experimental side in the near future at LHC. Quite remarkably the quantity N follows closely the Stefan Boltzmann limit N_{SB} for a massless noninteracting system which is given in Fig. 3 by the upper thin solid line and has the physical interpretation of a gluon density. Though N differs by less than 15% from the Stefan Boltzmann (SB) limit for $T > 2T_c$ the physical interpretation is essentially different! Whereas in the SB limit all gluons move on the light cone without interactions only a small fraction of gluons can be attributed to quasiparticles with density N^+ within the DQPM that propagate within the lightcone. The space-like part N^- corresponds to 'gluons' exchanged in t -channel scattering processes and thus cannot be propagated explicitly in off-shell transport approaches without violating causality and/or Lorentz invariance.

The scalar density N_s follows smoothly the time-like density N^+ as a function of temperature which can be explicitly seen in the lower part of Fig. 3 where the ratio N_s/N^+ is shown versus T/T_c . Consequently, the scalar density N_s uniquely relates to the time-like density N^+ or the temperature T in thermal equilibrium which will provide some perspectives for a transport theoretical treatment (see Section 3).

The separation of N^+ and N^- so far has no direct dynamical implications except for the fact that only the fraction N^+ can explicitly be propagated in transport as argued above. Thus we consider the energy densities,

$$T_{00}^{\pm}(T) = \tilde{\text{Tr}}^{\pm} \omega , \quad (14)$$

that specify time-like and space-like contributions to the quasiparticle energy density. It is worth pointing out that the quantity $T_{00} = T_{00}^+ + T_{00}^-$ in case of a conventional quasi-particle model with vanishing width γ in general is quite different from ϵ in (9) because the interaction energy density in this case is not included in (14), i.e.

$$T_{00} = T_{00}^+ = d_g \int d\omega \frac{d^3p}{(2\pi)^3} 2\omega \delta(\omega^2 - M^2 - \mathbf{p}^2) \Theta(\omega) \Theta(\pm P^2) n(\omega/T) \omega \quad (15)$$

since $\omega^2 - \mathbf{p}^2 = M^2 = P^2 > 0$ due to the mass-shell δ -function.

How does the situation look like in case of dynamical quasiparticles of finite width? To this aim we consider the integrand in the energy density (14) which reads as (in spherical momentum coordinates with angular degrees of freedom integrated out)

$$I(\omega, p) = \frac{d_g}{2\pi^3} p^2 \omega^2 \rho(\omega, p^2) n(\omega/T). \quad (16)$$

Here the integration is to be taken over ω and p from 0 to ∞ . The integrand $I(\omega, p)$ is shown in Fig. 4 for $T = 1.02T_c$ (l.h.s.) and $T = 2T_c$ (r.h.s.) in terms of contour lines. For the lower temperature the gluon mass is about 0.91 GeV and the width $\gamma \approx 0.15$ GeV such that the quasiparticle properties are close to a ρ -meson in free space. In this case the integrand $I(\omega, p)$ is essentially located in the time-like sector and the integral over the space-like sector is subdominant. This situation changes for $T = 2T_c$ where the mass is about 0.86 GeV while the width increases to $\gamma \approx 0.56$ GeV. As one observes from the r.h.s. of Fig. 4 the maximum of the integrand is shifted towards the line $\omega = p$ and higher momentum due to the increase in temperature by about a factor of two; furthermore, the distribution reaches far out in the space-like sector due to the Bose factor $n(\omega/T)$ which favors small ω . Thus the relative importance of the time-like (+) part to the space-like (-) part is dominantly controlled by the width γ - relative to the pole mass - which determines the fraction of T_{00}^- with negative invariant mass squared ($P^2 < 0$) relative to the time-like part T_{00}^+ .

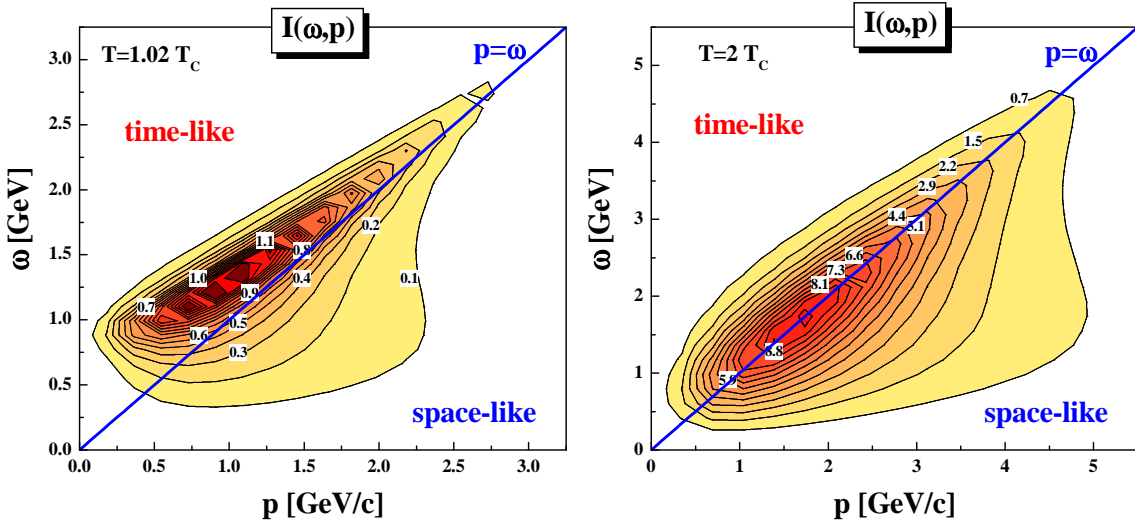


Fig. 4. The integrand $I(\omega, p)$ (16) for $T = 1.02T_c$ (l.h.s.) and $T = 2T_c$ (r.h.s.) in terms of contour lines. The straight (blue) line ($\omega = p$) separates the time-like from the space-like sector. Note that for a convergence of the energy density integral the upper limits for ω and p have to be increased by roughly an order of magnitude compared to the area shown in the figure.

The explicit results for the quasiparticle energy densities T_{00}^+ and T_{00}^- are displayed in Fig. 5 by the dashed blue and dot-dashed red lines (multiplied by $(T_c/T)^4$), respectively. As in case of N^+ and N^- the space-like energy density T_{00}^- is seen

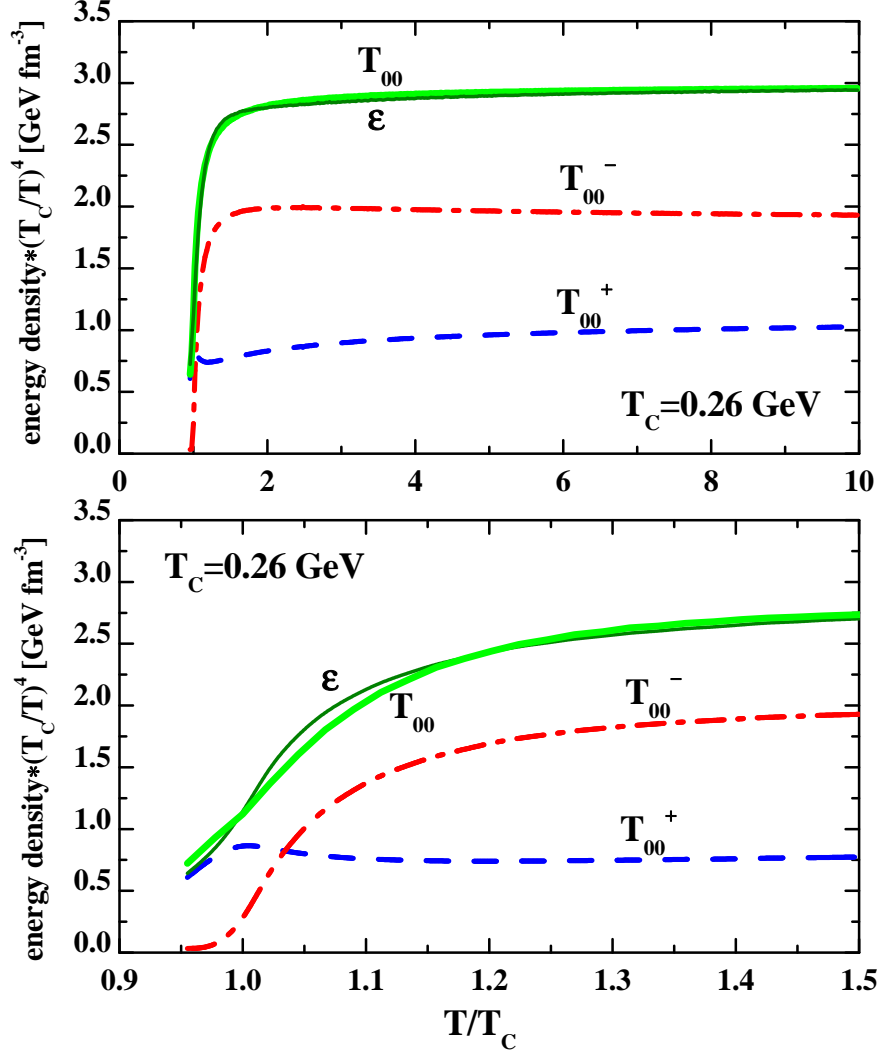


Fig. 5. Upper part: The time-like energy density T_{00}^+ (dashed blue line), the space-like energy density T_{00}^- (dot-dashed red line) and the total energy density $T_{00} = T_{00}^+ + T_{00}^-$ (thick solid green line) as a function of T/T_c . The thin black line displays the energy density $\epsilon(T/T_c)$ from (9); it practically coincides with T_{00} within the linewidth and is hardly visible. All densities are multiplied by the dimensionless factor $(T_c/T)^4$ in order to divide out the leading temperature dependence. Lower part: Same as the upper part in order to enhance the resolution close to T_c .

to be larger than the time-like part T_{00}^+ for all temperatures above $1.05 T_c$. Since the time-like part T_{00}^+ corresponds to the independent quasiparticle energy density within the lightcone, the space-like part T_{00}^- can be interpreted as an interaction density V if the quasiparticle energy T_{00} matches the total energy density $\epsilon(T)$ (9) as determined from the thermodynamical relations (8) and (9). In fact, the DQPM yields an energy density T_{00} - adding up the space-like and time-like parts - that almost coincides with $\epsilon(T)$ from (9) as seen in Fig. 5 where both quantities (multiplied by $(T_c/T)^4$) are displayed in terms of the thin black and thick solid green lines, respectively; actually both results practically coincide within the linewidth for $T > 2T_c$. An explicit representation of their numerical ratio gives unity within 2% for

$T > 2T_c$; the remaining differences can be attributed to temperature derivatives $\sim d/dT(\ln(\gamma/E))$ etc. in order to achieve thermodynamic consistency but this is not the primary issue here and will be discussed in a forthcoming study [42]. The deviations are more clearly visible close to T_c (lower part of Fig. 2) where the variation of the width and mass are most pronounced. However, for all practical purposes one may consider $T_{00}(T) \approx \epsilon(T)$ and separate the kinetic energy density T_{00}^+ from the potential energy density T_{00}^- as a function of T or - in equilibrium - as a function of the scalar gluon density N_s or N^+ , respectively.

3 Dynamics of time-like quasiparticles

Since in transport dynamical approaches there are no thermodynamical Lagrange parameters like the inverse temperature $\beta = T^{-1}$ or the quark chemical potential μ_q , which have to be introduced in thermodynamics in order to specify the average values of conserved quantities (or currents in the relativistic sense), derivatives of physical quantities with respect to the scalar density $\rho_s = N_s$ (or time-like gluon density $\rho_g = N^+$) are considered in the following (cf. Ref. [43]). As mentioned above one may relate derivatives in thermodynamic equilibrium via,

$$\frac{d}{dT} = \frac{d}{d\rho_s} \frac{d\rho_s}{dT}, \quad (17)$$

if the volume and pressure are kept constant. For example, a numerical evaluation of $d\rho_s/d(T/T_c)$ gives

$$\frac{d\rho_s}{d(T/T_c)} \approx a_1 \left(\frac{T}{T_c}\right)^{2.1} - a_2 \exp(-b(\frac{T}{T_c})) \quad (18)$$

with $b=5$, $a_1 = 1.5 fm^{-3}$ and $a_2 = 104 fm^{-3}$, which follows closely the quadratic scaling in T/T_c as expected in the Stefan Boltzmann limit. The additional exponential term in (18) provides a sizeable correction close to T_c . The approximation (18) may be exploited for convenient conversions between ρ_s and T/T_c in the pure gluon case but will not be explicitly used in the following.

The independent quasiparticle energy density $T_K := T_{00}^+$ and potential energy density $V := T_{00}^-$ now may be expressed as functions of ρ_s (or ρ_g) instead of the temperature T . The interaction energy density then might be considered as a scalar energy density which - as in the nonlinear σ -model for baryonic matter [44] - is a nonlinear function of the scalar density ρ_s . As in case of nuclear matter problems the scalar density ρ_s does not correspond to a conserved quantity when integrating over space; it only specifies the interaction density parametrically, i.e. $V(\rho_s)$. Alternatively one might separate V into parts with different Lorentz structure, e.g. scalar and vector parts

as in case of nuclear matter problems [44], but this requires additional information that cannot be deduced from the DQPM alone.

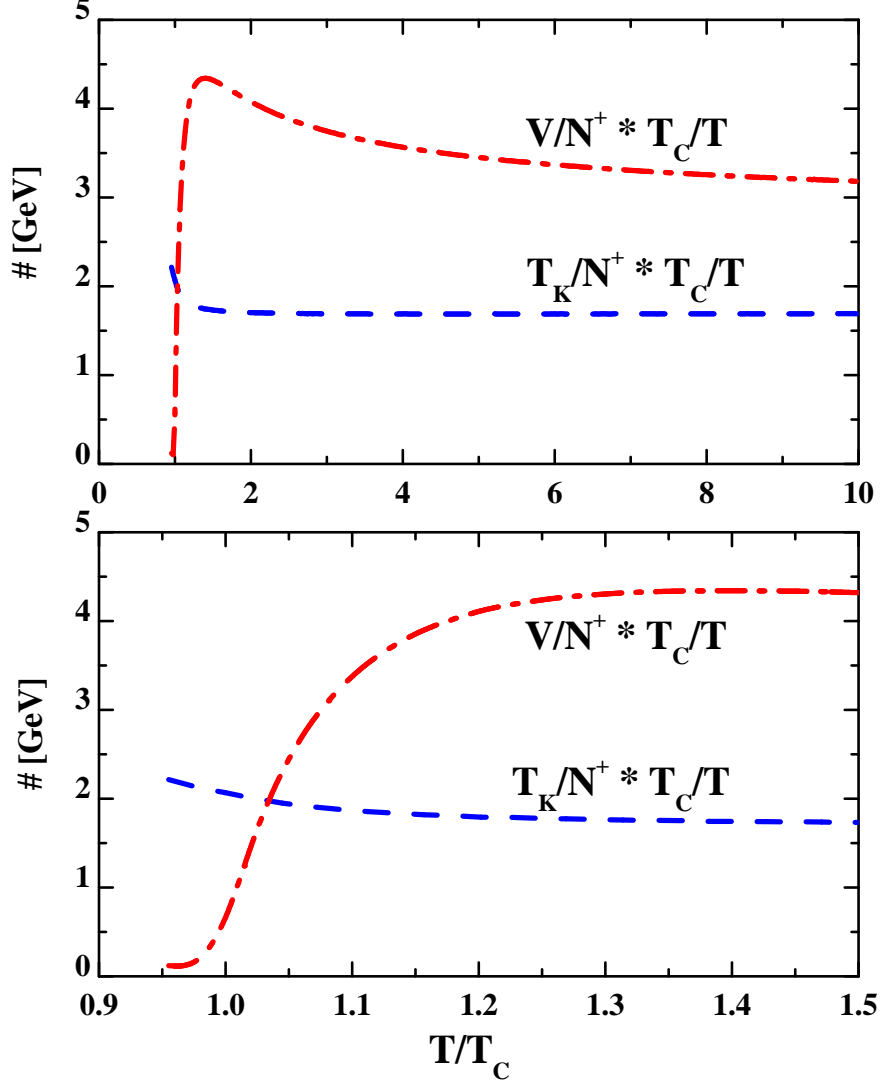


Fig. 6. Upper part: The quasiparticle energy per degree of freedom T_K/N^+ (dashed blue line) and the space-like potential energy per degree of freedom V/N^+ (dot-dashed red line) as a function of T/T_c . All energies are multiplied by the dimensionless factor (T_c/T) . Lower part: Same as the upper part in order to enhance the resolution close to T_c .

It is instructive to show the 'quasiparticle' and potential energy per degree of freedom T_K/N^+ and V/N^+ as a function of e.g. N^+ , N_s or T/T_c . As one might have anticipated the kinetic energy per effective degree of freedom is smaller than the respective potential energy for $T/T_c > 1.05$ as seen from Fig. 6 where both quantities are displayed as a function of T/T_c in terms of the dashed and dot-dashed line, respectively. It is seen that the potential energy per degree of freedom steeply rises in the vicinity of T_c whereas the independent quasiparticle energy rises almost linearly with T . Consequently rapid changes in the density - as in the expansion of the fireball in ultrarelativistic nucleus-nucleus collisions - are accompanied by a dramatic change in the potential energy density and thus to a violent acceleration of

the quasi-particles. It is speculated here that the large collective flow of practically all hadrons seen at RHIC [6] might be attributed to the early strong partonic forces expected from the DQPM.

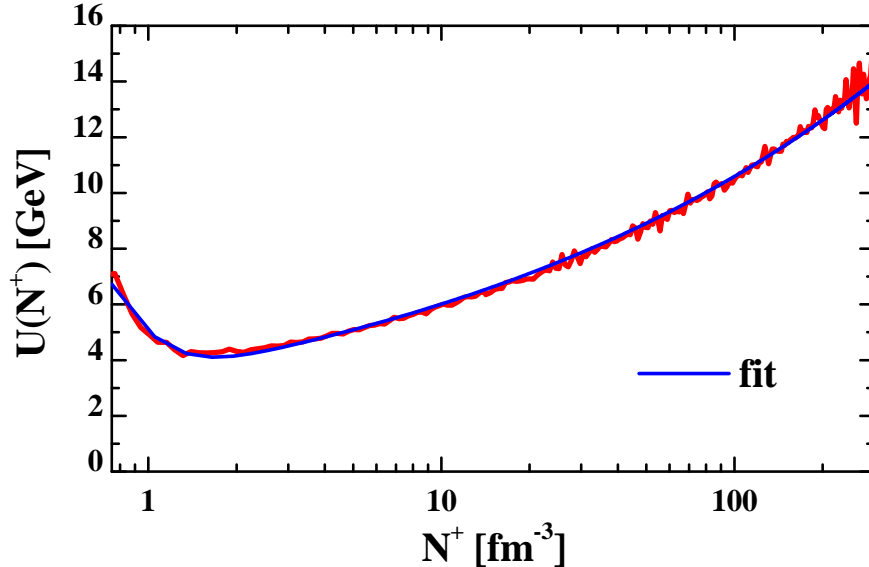


Fig. 7. The mean-field potential $U(N^+) = U(\rho_g)$ as a function of the time-like gluon density $N^+ = \rho_g$ in comparison to the fit (19) (solid blue line). The densities $N^+ = 1, 1.4, 5, 10, 50, 100 \text{ fm}^{-3}$ correspond to scaled temperatures of $T/T_c \approx 1.025, 1.045, 1.25, 1.5, 2.58, 3.25$, respectively (cf. Fig. 3).

In order to obtain some idea about the mean-field potential $U_s(\rho_s)$ (or $U(\rho_g)$ in the rest frame) one can consider the derivative $dV/\rho_s = U_s(\rho_s)$ or $dV/N^+ = U(N^+) = U(\rho_g)$. The latter is displayed in Fig. 7 as a function of $N^+ = \rho_g$ and shows a distinct minimum at $\rho_g \approx 1.4 \text{ fm}^{-3}$ which corresponds to a temperature $T \approx 1.045T_c$. The actual numerical results can be fitted by the expression,

$$U(\rho_g) = \frac{dV}{d\rho_g} \approx 39 e^{-\rho_g/0.31} + 2.93 \rho_g^{0.21} + 0.55 \rho_g^{0.36} \quad [\text{GeV}] , \quad (19)$$

where ρ_g is given in fm^{-3} and the actual numbers in front carry a dimension in order to match to the proper units of GeV for the mean-field U . By analytical integration of (19) one obtains a suitable approximation to $V(\rho_g)$. The approximation (19) works sufficiently well as can be seen from Fig. 7 - showing a comparison of the numerical derivative dV/dN^+ with the fit (19) in the interval $0.7 \text{ fm}^{-3} < N^+ \leq 300 \text{ fm}^{-3}$ - such that one may even proceed with further analytical calculations. Note that a conversion between the time-like quasiparticle density $N^+ = \rho_g$ and the scalar density ρ_s is easily available numerically (cf. lower part of Fig. 3) such that derivatives with respect to ρ_s are at hand, too; the latter actually enter the explicit transport calculations [45] while derivatives with respect to ρ_g in the rest frame of the system are more suitable for physical interpretation and will be used below.

Some information on the properties of the effective gluon-gluon interaction v_{gg} may be extracted from the second derivative of V with respect to ρ_g , i.e.

$$v_{gg}(\rho_g) := \frac{d^2V}{d\rho_g^2} \approx -125.8 e^{-\rho_g/0.31} + 0.615/\rho_g^{0.79} + 0.2/\rho_g^{0.64} \quad [\text{GeVfm}^3], \quad (20)$$

where the numbers in front have again a dimension to match the units of GeV fm^3 . The effective gluon-gluon interaction v_{gg} (20) is strongly attractive at low density $0.003 \text{ fm}^{-3} < \rho_g$ and changes sign at $\rho_g \approx 1.4 \text{ fm}^{-3}$ to become repulsive at higher densities. Note that the change of quasiparticle momenta (apart from collisions) will be essentially driven by the (negative) space-derivatives $-\nabla U(x) = -dU(\rho_g)/d\rho_g \nabla\rho_g(x)$ (or alternatively by $-dU_s(\rho_s)/d\rho_s \nabla\rho_s(x)$). This implies that the gluonic quasiparticles (at low gluon density) will bind with decreasing density, i.e. form 'glueballs' dynamically close to the phase boundary and repel each other for $\rho_g \geq 1.4 \text{ fm}^{-3}$. Note that color neutrality is imposed by color-current conservation and only acts as a boundary condition for the quantum numbers of the bound/resonant states in color space.

This situation is somehow reminiscent of the nuclear matter problem [44] where a change in sign of the 2nd derivative of the potential energy density of nuclear matter at low density indicates the onset of clustering of nucleons, i.e. to deuterons, tritons, α -particles etc., which form the states of the many-body system at low nucleon densities (and not a low density nucleon gas). This is easy to follow up for the simplified nonrelativistic energy density functional ϵ_N for nuclear matter,

$$\epsilon_N \approx A\rho_N^{5/3} + \frac{B}{2}\rho_N^2 + \frac{3C}{7}\rho_N^{7/3}, \quad (21)$$

where the first term gives the kinetic energy density and the second and third term correspond to attractive and repulsive interaction densities. For $A \approx 0.073 \text{ GeV fm}^2$, $B \approx -1.3 \text{ GeV fm}^3$ and $C \approx 1.78 \text{ GeV fm}^4$ a suitable energy density for nuclear matter is achieved; it gives a minimum in the energy per nucleon $E/A = \epsilon_N/\rho_N \approx -0.016 \text{ GeV}$ for nuclear saturation density $\rho_N^0 \approx 0.168 \text{ fm}^{-3}$. The mean-field potential $U_N = B\rho_N + C\rho_N^{4/3}$ has a minimum close to ρ_N^0 such that the effective nucleon-nucleon interaction strength $v_{NN} = B + 4/3C\rho_N^{1/3}$ changes from attraction to repulsion at this density. Note that in the gluonic case the minimum in the mean-field potential U (19) occurs at roughly 8 times ρ_N^0 and the strength of the gluonic interaction is higher by more than 2 orders of magnitude!

The confining nature of the effective gluon-gluon interaction v_{gg} (20) becomes apparent in the limit $\rho_g \rightarrow 0$, where the huge negative exponential term dominates for $\rho_g > 0.003 \text{ fm}^{-3}$; for even smaller densities the singular repulsive terms take over. Note, however, that the functional extrapolation of the fit (19) to vanishing gluon density ρ_g has to be considered with care and it should only be concluded that the interaction strength becomes 'very large'. On the other hand the limit $\rho_g \rightarrow 0$ is only

academical because the condensation/fusion dynamically occurs for $\rho_g \approx 1 \text{ fm}^{-3}$.

A straight forward way to model the gluon condensation or clustering to confined glueballs dynamically (close to the phase transition) is to adopt a screened Coulomb-like potential $v_c(r, \Lambda)$ with the strength $\int d^3r v_c(r, \Lambda)$ fixed by $v_{gg}(\rho_g)$ from (20) and the screening length Λ from IQCD studies. For the 'dilute gluon regime' ($\rho_g < 1.4 \text{ fm}^{-3}$), where two-body interactions should dominate, one may solve a Schrödinger (or Klein-Gordon) equation for the bound and/or resonant states. This task is not addressed further in the present study since for the actual applications (as in the Parton-Hadron-String-Dynamics (PHSD) approach [45]) dynamical quark and antiquarks have to be included. The latter degrees of freedom do not change the general picture very much for higher temperatures $T > 2T_c$ but the actual numbers are different close to T_c since the quarks and antiquarks here dominate over the gluons due to their lower mass. The reader is referred to an upcoming study in Ref. [42].

Some comments on expanding gluonic systems in equilibrium appear in place, i.e. for processes where the total volume \tilde{V} and pressure P play an additional role. For orientation we show the entropy per time-like particle s/N^+ in Fig. 8 as a function of N^+ (upper) and T/T_c (lower part) which drops close to the phase boundary since the quasiparticles become weakly interacting (cf. Fig. 6). Note that this is essentially due to the low density and not due to the interaction strength (20); a decrease of the width γ (as encoded in (5)) implies a decrease in the interaction rate! An expansion process with conserved total entropy $S = s\tilde{V}$ leads to a change in the total gluon number $N^+\tilde{V}$ since s/N^+ changes with density (or temperature) (Fig. 8). The same holds for an expansion process with constant total energy $\epsilon\tilde{V}$ since also ϵ/N^+ is varying with density (or temperature). Other scenarios involving e.g. $S = P/T$ also involve a change of the gluon number $N^+\tilde{V}$ during the cooling process such that reactions like $gg \leftrightarrow g$, $ggg \leftrightarrow gg$ etc. are necessary ingredients of any transport theoretical approximation. We do not further investigate different expansion scenarios here since the reactions $g \leftrightarrow q\bar{q}$, i.e. the gluon splitting to a quark and antiquark as well as the backward fusion process, are found to play a dominant role in the vicinity of the phase transition as well as for higher temperatures [42,45].

4 Conclusions and discussion

The present study has provided a novel interpretation of the dynamical quasiparticle model (DQPM) by separating time-like and space-like quantities for 'particle densities', energy densities, entropy densities ect. that also paves the way for an off-shell transport approach [45]. The entropy density s in (7) is found to be dominated by the on-shell quasiparticle contribution (first line in (7)) (cf. [31]) while the space-like part of the off-shell contribution (second line in (7)) gives only a small (but important) enhancement (cf. Fig. 2). However, in case of the 'gluon density' $N = N^+ + N^-$ and the gluon energy density $T_{00} = T_{00}^+ + T_{00}^-$ the situation is opposite: here the space-like

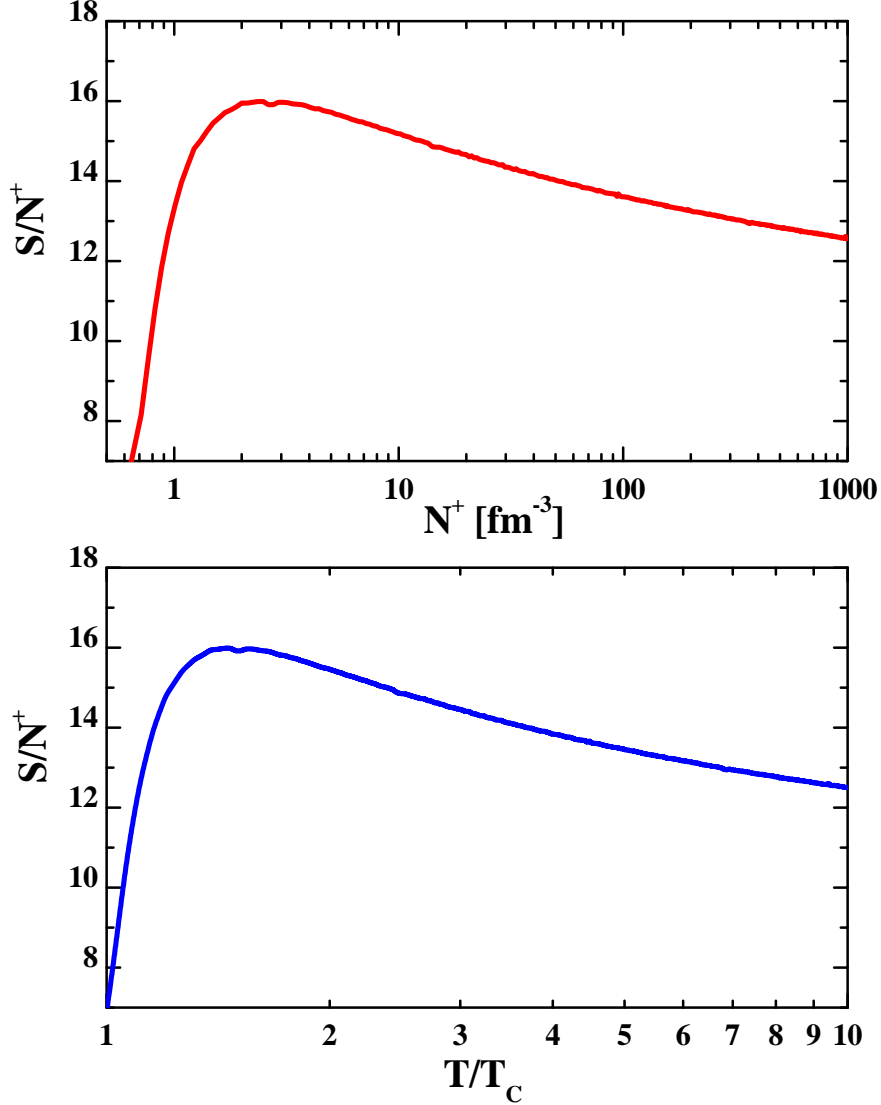


Fig. 8. The entropy per degree of freedom s/N^+ as a function of N^+ (upper part) or T/T_c (lower part).

parts (N^-, T_{00}^-) dominate over the time-like parts (N^+, T_{00}^+) except close to T_c where the independent quasiparticle limit is approximately regained. The latter limit is a direct consequence of the infrared enhancement of the coupling (4) close to T_c (in line with the IQCD studies in Ref. [36]) and a decrease of the width γ (5) when approaching T_c from above.

Since only the time-like part N^+ can be propagated within the lightcone the space-like part N^- has to be attributed to t -channel exchange gluons in scattering processes that contribute also to the space-like energy density T_{00}^- . The latter quantity may be regarded as potential energy density V . This, in fact, is legitimate since the quasiparticle energy density T_{00} very well matches the energy density (9) obtained from the thermodynamical relations. Only small deviations close to T_c indicate that the DQPM in its straightforward application is not thermodynamically consistent. However, by accounting for 'rearrangement terms' in the energy density - as known

from the nuclear many-body problem [46] - full thermodynamical consistency may be regained [42].

It is instructive to compare the present DQPM to other recent models. In the PNJL² model [47] the gluonic pressure is build up by a constant effective potential $U(\Phi, \Phi^*; T)$ which controls the thermodynamics of the Polyakov loop Φ . It is expanded in powers of $\Phi\Phi^*$ with temperature dependent coefficients in order to match lQCD thermodynamics. Thus in the PNJL there are no time-like gluons; the effective potential $U(\Phi, \Phi^*; T)$ stands for a static gluonic pressure that couples to the quark/antiquark degrees of freedom. The latter are treated in mean-field approximation, i.e. without dynamical width, whereas the DQPM incorporates a sizeable width γ .

Another approach to model lQCD thermodynamics has been suggested in Ref. [43] and is based on an effective Lagrangian which is nonlinear in the effective quark and gluon fields. In this way the authors avoid a parametrization of the interaction density in terms of Lagrange parameters (T, μ) and achieve thermodynamical consistency. The latter approach is closer in spirit to the actual interpretation of the DQPM and may be well suited for an on-shell transport theoretical formulation. The on-shell restriction here comes about since effective Lagrangian approaches should only be evaluated in the mean-field limit which implies vanishing scattering width for the quasiparticles. This is sufficient to describe systems in thermodynamical equilibrium, where forward and backward interaction rates are the same, but might not provide the proper dynamics out-of-equilibrium.

Some note of caution with respect to the present DQPM appears appropriate: the parameters in the effective coupling (4) and the width (5) have been fixed in the DQPM by the entropy density (7) to lQCD results assuming the form (2) for the spectral function $\rho(\omega)$. Alternative assumptions for $\rho(\omega)$ will lead to slightly different results for the time-like density, energy densities *etc.* but not to a qualitatively different picture. Independent quantities from lQCD should allow to put further constraints on the more precise form of $\rho(\omega)$ such as calculations for transport coefficients [16]; unfortunately such lQCD studies are only at the beginning. A more important issue is presently to extend the DQPM to incorporate dynamical quark and antiquark degrees of freedom (as in [31]) in order to catch the physics of gluon splitting and quark-antiquark fusion ($g \leftrightarrow q + \bar{q}$, $g + g \leftrightarrow q + \bar{q} + g$) reactions [42,45].

Coming back to the questions raised in the Introduction concerning i) the appropriate description of QCD thermodynamics within the DQPM and ii) the possibility to develop a consistent off-shell partonic transport approach as well as iii) the perspectives for a dynamical description of the transition from partonic to hadronic degrees of freedom, we are now in the position to state: most likely 'Yes'.

² Polyakov-loop-extended Nambu Jona-Lasinio

The author acknowledges valuable discussions with E. L. Bratkovskaya and A. Peshier. Furthermore he likes to thank S. Leupold for a critical reading of the manuscript and constructive suggestions.

References

- [1] *Quark Matter 2002*, Nucl. Phys. A 715 (2003) 1; *Quark Matter 2004*, J. Phys. G 30 (2004) S633; *Quark Matter 2005*, Nucl. Phys. A 774 (2006) 1.
- [2] F. Karsch *et al.*, Nucl. Phys. B 502 (2001) 321.
- [3] M. H. Thoma, J. Phys. G 31 (2005) L7; Nucl. Phys. A 774 (2006) 307.
- [4] A. Peshier and W. Cassing, Phys. Rev. Lett. 94 (2005) 172301.
- [5] E. Shuryak, Prog. Part. Nucl. Phys. 53 (2004) 273.
- [6] I. Arsene *et al.*, Nucl. Phys. A 757 (2005) 1; B. B. Back *et al.*, Nucl. Phys. A 757 (2005) 28; J. Adams *et al.*, Nucl. Phys. A 757 (2005) 102; K. Adcox *et al.*, Nucl. Phys. A 757 (2005) 184.
- [7] T. Hirano and M. Gyulassy, Nucl. Phys. A 769 (2006) 71.
- [8] W. Cassing, K. Gallmeister, and C. Greiner, Nucl. Phys. A 735 (2004) 277.
- [9] E. L. Bratkovskaya *et al.*, Phys. Rev. C 67 (2003) 054905; Phys. Rev. C 69 (2004) 054907; Phys. Rev. C 71 (2005) 044901.
- [10] K. Gallmeister and W. Cassing, Nucl. Phys. A748 (2005) 241.
- [11] P. Kolb and U. Heinz, nucl-th/0305084, in 'Quark Gluon Plasma 3', Eds. R. C. Hwa and X.-N. Wang, World Scientific, Singapore, 2004.
- [12] C. Nonaka and S. A. Bass, Phys. Rev. C 75 (2007) 014902; Nucl. Phys. A 774 (2006) 873.
- [13] G. E. Brown, C.-H. Lee, M. Rho, and E. Shuryak, Nucl. Phys. A740 (2004) 171.
- [14] G. E. Brown, C.-H. Lee, and M. Rho, Nucl. Phys. A 747 (2005) 530.
- [15] E. V. Shuryak and I. Zahed, Phys. Rev. D 70 (2004) 054507.
- [16] A. Nakamura and S. Sakai, Phys. Rev. Lett. 94 (2005) 072305; Nucl. Phys. A 774 (2006) 775.
- [17] E. L. Bratkovskaya and W. Cassing, Nucl. Phys. A 619 (1997) 413; W. Cassing and E. L. Bratkovskaya, Phys. Rept. 308 (1999) 65.
- [18] S.A. Bass *et al.*, Prog. Part. Nucl. Phys. 42 (1998) 279.
- [19] M. Bleicher *et al.*, J. Phys. G 25 (1999) 1859.
- [20] K. Geiger, Phys. Rep. 258 (1995) 237.

- [21] B. Zhang, M. Gyulassy, and C. M. Ko, Phys. Lett. B 455 (1999) 45.
- [22] D. Molnar and M. Gyulassy, Phys. Rev. C 62 (2000) 054907; Nucl. Phys. A 697 (2002) 495; Nucl. Phys. A 698 (2002) 379.
- [23] S. A. Bass, B. Müller, and D. K. Srivastava, Phys. Lett. B 551 (2003) 277; Acta Phys. Hung. A 24 (2005) 45.
- [24] Z.-W. Lin *et al.*, Phys. Rev. C 72 (2005) 064901.
- [25] Z. Xu and C. Greiner, Phys. Rev. C 71 (2005) 064901; Nucl. Phys. A 774 (2006) 034909.
- [26] W. Cassing and S. Juchem, Nucl. Phys. A 665 (2000) 417; Nucl. Phys. A 672 (2000) 417.
- [27] S. Juchem, W. Cassing, and C. Greiner, Phys. Rev. D 69 (2004) 025006; Nucl. Phys. A 743 (2004) 92.
- [28] S. Leupold, Nucl. Phys. A 672 (2000) 475.
- [29] W. Cassing, L. Tolos, E. L. Bratkovskaya, and A. Ramos, Nucl. Phys. A 727 (2003) 59.
- [30] A. Peshier, Phys. Rev. D 70 (2004) 034016.
- [31] A. Peshier, J. Phys. G 31 (2005) S371.
- [32] F. Karsch, Nucl. Phys. A 698 (2002) 199c; F. Karsch, E. Laermann and A. Peikert, Phys. Lett. B 478 (2000) 447.
- [33] J. P. Blaizot, E. Iancu, and A. Rebhan, Phys. Rev. D 63 (2001) 065003.
- [34] A. Peshier, B. Kämpfer, O.P. Pavlenko, and G. Soff, Phys. Rev. D 54 (1996) 2399; P. Levai, U. Heinz, Phys. Rev. C 57 (1998) 1879; A. Peshier, B. Kämpfer, G. Soff, Phys. Rev. C 61 (2000) 045203, Phys. Rev. D 66 (2002) 094003.
- [35] J. Letessier and J. Rafelski, Phys. Rev. C 67 (2003) 031902.
- [36] O. Kaczmarek, F. Karsch, F. Zantow, and P. Petreczky, Phys. Rev. D 70 (2004) 074505; erratum-ibid. D 72 (2005) 059903.
- [37] R. D. Pisarski, Phys. Rev. Lett. 63 (1989) 1129; V. V. Lebedev and A. V. Smilga, Ann. Phys. (N.Y.) 202 (1990) 229.
- [38] A. Peshier, Phys. Rev. D 63 (2001) 105004.
- [39] M. Okamoto *et al.*, Phys. Rev. D 60 (1999) 094510.
- [40] G. Boyd *et al.*, Nucl. Phys. B 469 (1996) 419.
- [41] W. Cassing, E. L. Bratkovskaya, and S. Juchem, Nucl. Phys. A 674 (2000) 249.
- [42] W. Cassing, to be published
- [43] Yu.B. Ivanov, V.V. Skolov, and V.D. Toneev, Phys. Rev. D 71 (2005) 014005.

- [44] B. D. Serot and J. D. Walecka, *Adv. Nucl. Phys.* 16 (1986) 1; B. D. Serot, *Rep. Prog. Phys.* 55 (1992) 1855; P. G. Reinhard, *Rep. Prog. Phys.* 52 (1989) 439.
- [45] W. Cassing, talk at ECT*, Workshop on *Parton Propagation through Strongly Interacting Matter*, September 27, 2005, [<http://conferences.jlab.org/ECT/program>].
- [46] C. Fuchs, H. Lenske, and H. H. Wolter, *Phys. Rev. C* 52 (1995) 3043.
- [47] C. Ratti, M. A. Thaler and W. Weise, *Phys. Rev. D* 73 (2006) 014019; C. Ratti and W. Weise, *Phys. Rev. D* 70 (2004) 054013.